Published in final edited form as:
*Neurobiol Dis*. 2012 February ; 45(2): 671–682. doi:10.1016/j.nbd.2011.10.006.

# The NMDA receptor co-agonists, D-serine and glycine, regulate neuronal dendritic architecture in the somatosensory cortex

**Darrick T. Balu**[a,b], **Alo C. Basu**[a,b], **John P. Corradi**[c], **Angela M. Cacace**[c], and **Joseph T. Coyle**[a,b,*]

[a]Department of Psychiatry, Harvard Medical School, Boston, MA USA

[b]Laboratory for Psychiatric and Molecular Neuroscience, McLean Hospital, Belmont, MA, USA

[c]Neuroscience Biology & Applied Genomics, Bristol-Myers Squibb Research and Development, Wallingford, CT, USA

## Abstract

There is substantial evidence, both pharmacological and genetic, that hypofunction of the N-methyl-D-aspartate receptor (NMDAR) is a core pathophysiological feature of schizophrenia. There are morphological brain changes associated with schizophrenia, including perturbations in the dendritic morphology of cortical pyramidal neurons and reduction in cortical volume. Our experiments investigated whether these changes in dendritic morphology could be recapitulated in a genetic model of NMDAR hypofunction, the serine racemase knockout (SR−/−) mouse. Pyramidal neurons in primary somatosensory cortex (S1) of SR−/− mice had reductions in the complexity, total length, and spine density of apical and basal dendrites. In accordance with reduced cortical neuropil, SR−/− mice also had reduced cortical volume as compared to wild type mice. Analysis of S1 mRNA by DNA microarray and gene expression analysis revealed gene changes in SR−/− that are associated with psychiatric and neurologic disorders, as well as neurodevelopment. The microarray analysis also identified reduced expression of brain derived neurotrophic factor (BDNF) in SR−/− mice. Follow-up analysis by ELISA confirmed a reduction of BDNF protein levels in the S1 of SR−/− mice. Finally, S1 pyramidal neurons in glycine transporter heterozygote (GlyT1+/−) mutants, which display enhanced NMDAR function, had increased dendritic spine density. These results suggest that proper NMDAR function is important for the arborization and spine density of pyramidal neurons in cortex. Moreover, they suggest that NMDAR hypofunction might, in part, be contributing to the dendritic and synaptic changes observed in schizophrenia and highlight this signaling pathway as a potential target for therapeutic intervention.

### Keywords

serine racemase; glycine; NMDA receptor; somatosensory cortex; BDNF; dendritic spines; schizophrenia



*Corresponding author: Joseph T. Coyle, M.D., Harvard Medical School, McLean Hospital, 115 Mill Street, Belmont, MA 02478, USA., joseph_coyle@hms.harvard.edu, Tel.: 617-855-2101, Fax: 617-855-2705.

## Introduction

Schizophrenia is a complex mental disorder that is clinically characterized by positive symptoms, negative symptoms, and cognitive deficits. Over the past two decades, there has been converging evidence supporting the hypothesis that N-methyl-D-aspartate receptor (NMDAR) hypofunction is a key component in the etiology of schizophrenia (Coyle, 2006; Javitt and Zukin, 1991; Krystal et al., 1994; Tsai et al., 1995).

Activation of NMDARs requires the binding of either glycine or D-serine at the glycine modulatory site (GMS) on the NR1 subunit (Kishi and Macklis, 2004). D-Serine is enriched in corticolimbic regions of the brain, where its localization closely parallels that of NMDARs (Schell et al., 1995). The finding that D-serine is decreased in cerebrospinal fluid and serum samples from individuals with schizophrenia (Hashimoto et al., 2005a; Hashimoto et al., 2003) is consistent with the hypothesis that lower D-serine is part of the pathophysiology of the disorder. A single nucleotide polymorphism (SNP) in the gene encoding serine racemase (SR), the enzyme that produces D-serine from L-serine, has also been associated with schizophrenia (Morita et al., 2007). This mutation results in reduced expression of SR protein. *G72*, the gene product of which regulates D-serine levels by modulating the activity of D-amino acid oxidase (Sacchi et al., 2008), has been implicated as a risk gene for schizophrenia (Bass et al., 2009; Shi et al., 2008). A recent meta-analysis found that treatment with GMS agonists, including D-serine, exerted significant therapeutic effects on multiple symptom domains in schizophrenia (Tsai and Lin 2010).

In addition to modified GMS occupancy, NMDAR hypofunction in schizophrenia could also be due to postsynaptic deficits in NMDAR-mediated signaling. Although the findings in *postmortem* studies of NMDAR transcripts and protein expression levels in schizophrenia have been modest and inconsistent (Lewis and Gonzalez-Burgos, 2008), recent evidence suggests that other components of NMDAR signaling, as well as receptor processing and trafficking might be affected in the illness (Kristiansen et al., 2010a; Kristiansen et al., 2010b). Moreover, *postmortem* studies indicate that the endogenous NMDAR antagonists, kynurenic acid and N-acetyl-aspartyl glutamate are elevated in schizophrenia (Erhardt et al., 2007; Tsai et al., 1995).

*Postmortem* and imaging studies have revealed that in schizophrenia there is decreased cortical volume (Rasser et al., 2009) and widespread reduction in cortical thickness (Goldman et al., 2009). Since these volumetric reductions are associated with increased cell packing density, but not changes in neuronal number, they are likely due to decreased amounts of cortical neuropil (Selemon and Goldman-Rakic, 1999). In support of this hypothesis, somal volume, dendritic expanse and spine density of pyramidal neurons are reduced in several disparate cortical regions including sensory cortex of patients with schizophrenia (Garey et al., 1998; Glantz and Lewis, 2000; Kalus et al., 2000; Rajkowska et al., 1998; Sweet et al., 2010). Electrophysiological studies with subjects with schizophrenia demonstrate impairments in higher order processing of sensory information consistent with reduced connectivity (Javitt, 2009).

NMDARs have been well established to regulate dendritic elaboration and spine formation in the developing nervous system (Kwon and Sabatini, 2011). The process is complex, involving many downstream participants as well as interactions with neurotrophic factors (Lu, 2003; Sepulveda et al., 2010). Interestingly, under conditions of stress, NMDARs serve an opposite role, promoting atrophy of apical dendrites (Martin and Wellman, 2011). Much of the evidence of the role NMDARs play in dendritic maturation is derived from sub-acute manipulation of their expression or exposure to antagonists; but there is little information

about the effects of constitutive hypofunction of NMDARs, a condition analogous to schizophrenia.

In a preliminary study addressing a cognitive task requiring the frontal cortex, we found that mice lacking serine racemase (SR−/−), which exhibit reduced NMDAR activity, were cognitively impaired and had pyramidal neurons in the prefrontal cortex with reduced apical dendritic complexity. In the present study, we have carried out an extensive analysis of the dendritic structure of the pyramidal neurons in the intermediate layers of the primary sensory cortex in the SR−/− mice, focusing on the role of NMDARs.

## Materials and Methods

### Animals

SR−/− mice (Basu et al., 2009) and GlyT1 +/− mice (Tsai et al., 2004) were generated as previously described. Mice with a serine racemase null mutation resulting from targeted deletion of the first coding exon and mice with a glycine transporter 1 null mutation resulting from targeted deletion of exons 2–3 were backcrossed for over 10 generations onto a C57BL/6J background. SR+/− sires and dams were bred to produce wild-type (WT), as well as SR−/−offspring. GlyT1+/− sires or dams were bred to WT C57BL6/J animals to produce WT and GlyT1+/− offspring (GlyT1−/− mice die within 12h of birth due to respiratory failure). Adult male mice were used for all the experiments in this study. Animals were housed in groups of four in polycarbonate cages and maintained on a 12:12 h light/dark cycle in a temperature (22°C) and humidity controlled vivarium. Animals were given access to food and water *ad libitum*. All animal procedures were approved by the McLean Hospital Institutional Animal Care and Use Committee.

### Golgi staining

Golgi-staining was performed on adult (n = 5–6 mice/genotype) using the FD Rapid GolgiStain Kit (FD NeuroTechnologies, Ellicot City, MD) according to the manufacturer's instructions. Brains were removed, immersed in fixative (5 ml; equal volume of Solutions A:B) for 40 hours, and then transferred into Solution C and stored at 4°C until slicing. The fixed brains were sliced on a freezing microtome (American Optical 860, Buffalo, NY) at a thickness of 120 μm. Sections were mounted with Solution C on 3% gelatin-coated slides (75×25 mm; FD NeuroTechnologies, Ellicot City, MD). Excess Solution C was immediately removed from the slide using a Pasteur pipette and a fine paintbrush. Sections were kept at room temperature overnight, protected from light. Slides were then stained, dehydrated, and cleared with xylenes according to the manufacturer's protocol, without counterstaining.

### Quantification of dendritic morphology

Pyramidal neurons in the primary somatosensory cortex (S1) were chosen for reconstruction. Neurons were located in cortical layers II-IV between approximately 0.46 mm to 1.82 mm posterior to bregma (Paxinos & Franklin, 2001). Neurons selected for reconstruction were located in the middle third of the section. Neurons that were obscured by neighboring neurons and/or glia were excluded from analysis. Within each region examined, 3–8 neurons were reconstructed for each mouse. Neurons were traced at 40x on a Zeiss Axioskop40 microscope, and the morphology of apical and basilar arbors was quantified in three dimensions using Neurolucida (MBF Bioscience, Williston, VT). The experimenter was blind to genotype during tracing. Sholl analysis was performed using the Neurolucida Explorer software to assess dendritic complexity (concentric circles increased in diameter by 10 μm increments).

### Spine density analysis

Spines were counted on dendritic branches from 3–5 neurons per region in each animal. For apical dendrites, spines were counted on the apical trunk (last 40 μm) and oblique segments separately, because spine density has been shown to vary across these dendritic compartments (Peters and Kaiserman-Abramof, 1970). Neurons from SR−/− mice were visualized at 63x (oil-immersion) using a Leitz Laborlux12 microscope. One to two basilar branches at each order were selected and spines were counted using BioQuant Nova Prime software (BioQuant Image Analysis Corp., Nashville, TN). Dendrites from GlyT1+/− mice were visualized at 100x (oil-immersion) on a Zeiss Axioskop40 microscope. Spines were counted on branches from the same neurons that were reconstructed at 40x for dendritic analysis.

### Analysis of spine maturity

Using a 100x objective on a Ziess Axioskop40 microscope, spine morphology (number of spines- WT: 320; SR−/−: 250) was assessed on oblique apical branches and on the apical trunk of pyramidal neurons (2–3 mice/genotype; 6 cells/genotype) in the S1 barrel cortex. These were the same neurons that were used for measuring spine density. Spines were classified as morphologically immature (Types A–D) or mature (Types E–H) using previously described criteria (Galvez and Greenough, 2005).

### Nissl staining and cortical volume measurement

Brains from WT (n = 17) and SR−/− (n = 20) were removed, postfixed in 2% formaldehyde (1 week), and cryoprotected in 30% sucrose. Brains were exhaustively sectioned (160 μm) on a freezing microtome, with the position of the first cut for each brain randomly selected as to ensure systematic uniform random sampling. Every third section was mounted on gelatin-coated slides and stained using 0.1% cresylecht violet solution (pH 3.5). Cortical volume was estimated at 4x on a Zeiss Axioskop40 by the Cavalieri method (800 μm grid size; 14–18 sections per brain) using Stereo Investigator software (MBF Bioscience, Williston, VT). The grid size chosen estimated volumes with high precision (coefficient of error: 0.005).

### Cytochrome oxidase immunohistochemistry and analysis of posteromedial barrel subfield (PMBSF) of the somatosensory cortex

Brains from WT (n = 8) and SR−/− (n = 10) mice were removed and placed in a Braintree Scientific acrylic mouse brain matrix (1 mm section coronal; Braintree, MA). A 4mm block (approximately bregma 1.5mm to −2.5mm) was taken and all subcortical structures, as well as ventral cortex, were removed. The remaining tissue was fixed for several hours in 4% formaldehyde dissolved in 0.1M phosphate buffer (PB, pH 7.4). The cortices were then placed overnight in between glass microscope slides to facilitate flattening, and transferred to plastic immunohistochemistry slide staining jars that were filled with 4% formaldehyde solution. The cortices were then cryoprotected in 30% sucrose for 24h. The flatted brains were sectioned (80 μm) on a freezing microtome. The free-floating sections were then stained for cytochrome oxidase using 0.1M phosphate buffered saline (PBS) solution (pH 7.4) containing: 32.4 μM cytochrome c (Sigma Aldrich; St. Louis MO), 146 mM sucrose (Fisher Scientific; Fair Lawn, NJ), and 2.08mM DAB (Sigma Aldrich; St. Louis MO). The solution was stirred for approximately 1.5h and then passed through a 0.45 μm filter. Sections were incubated at 35° C for 3h on a shaker, after which Millipore water was added to stop the reaction. Sections were mounted on gelatin-coated slides, dehydrated with ethanol (70%, 80%, 95%, 100%; 5 min each), and cleared with xylenes (5 min).

Barrels in the PMBSF (rows D (2–9) and E (1–9)) were visualized on a Zeiss Axioskop40 microscope (4x magnification) and reconstructed using the area estimator function in Stereo Investigator (MBF Bioscience, Williston, VT). All of the individual barrels in these two rows were traced and their areas summed to give an aggregate intrabarrel area. The total area within the outline of rows D and E was also traced. The intrabarrel area was subtracted from the total area to determine the area between rows (interbarrel area).

### RNA isolation and collection of microarray data

RNA was isolated from tissue sections from wild-type (WT) and SR−/− mice (n = 6/genotype) using RNeasy mini kit (Qiagen, Valencia, CA) following manufacturer's recommendations. The quality of the total RNA from the those samples was monitored by the Agilent 2100 Bioanalyzer (Agilent Technologies, Palo Alto, CA) and RNA quantity was measured with a NanoDrop (NanoDrop Technologies, Inc. Wilmington, DE) following the manufacturer's instructions. All RNA samples including biological replicates were arrayed into 96 well microtiter plates following a randomized design format. All labeling reagents, GeneChip® HT One-Cycle Target Labeling kit, were purchased from Affymetrix (Santa Clara, CA). Double-stranded cDNAs were synthesized from 1 ug total RNA through reverse transcription with an oligo-dT primer containing the T7 RNA polymerase promoter and double strand conversion using the cDNA Synthesis System. Biotin-labeled cRNA was generated from the cDNA for hybridization to the arrays. All cRNA preparation steps were processed on a Caliper GeneChip Array Station from Affymetrix. Labeled cRNA were hybridized on Affymetrix mouse Genome HT_MG-430A arrays that contains >22,600 probe sets to analyze the expression of >14,000 mouse genes. Array hybridization, washing and scanning were performed according to the manufacturer's recommendations. Scanned images were subjected to visual inspection and a chip quality report was generated by the Affymetrix's GeneChip Operating System (GCOS) and Expression console (Affymetrix). The image data was processed using the Affymetrix GCOS algorithm utilizing quantile normalization to determine the specific hybridizing signal for each gene.

### Microarray data analysis

Microarray expression data were analyzed using dChip software (Li and Wong, 2001). Changes in gene expression were considered significant if $p < 0.05$ and the absolute value | fold-change| > 1.2, with the empirical false discovery rate estimated by permutation. The genes in which expression changes were significantly different between WT and SR−/− mice were then uploaded into Ingenuity Pathways Analysis (Ingenuity® Systems, www.ingenuity.com) software for the following analyses:

**Network generation—**Our data set containing gene identifiers and corresponding expression values of only significantly changes genes was uploaded into in the application. Each identifier was mapped to its corresponding object in Ingenuity's Knowledge Base. These molecules, called Network Eligible molecules, were overlaid onto a global molecular network developed from information contained in the Knowledge Base. Networks of Network Eligible Molecules were then algorithmically generated based on their functional connectivity.

**Functional Analysis of the Data Set as a whole—**The Functional Analysis identified the biological functions and/or diseases that were most significant to the data set. Molecules from the dataset were associated with biological functions and/or diseases in Ingenuity's Knowledge Base were considered for the analysis. B–H multiple testing correction was used to calculate a p-value determining the probability that each biological function and/or disease assigned to that data set is due to chance alone.

**Path Designer Graphical Representation—**Molecules are represented as nodes, and the biological relationship between two nodes is represented as an edge (line). All edges are supported by at least 1 reference from the scientific literature, from a textbook, or from canonical information stored in the Ingenuity Pathways Knowledge Base. Human, mouse, and rat orthologs of a gene are stored as separate objects in the Ingenuity Pathways Knowledge Base, but are represented as a single node in the network. The intensity of the node color indicates the degree of up- (red) or down- (green) regulation. Nodes are displayed using various shapes that represent the functional class of the gene product. Edges are displayed with various labels that describe the nature of the relationship between the nodes.

## RT-qPCR

Brains from adult (10–11 weeks old) WT and SR−/− mice independent from those used for the microarray study were dissected using a Zivic stainless steel adult mouse brain slicer (1mm section coronal; Zivic Instruments; Pittsburgh, PA). Two 1mm slices were obtained that corresponded approximately to 0.7mm to −0.8mm bregma. Using a mouse brain atlas as a guide, the S1 cortical regions were dissected from the two slabs and stored in RNAlater solution (Ambion; Austin, TX). RNA was isolated from the tissue samples using the miRvana miRNA isolation kit (Ambion; Austin, TX) according to the manufacturer's instructions. RNA concentration and quality was determined by placing the samples in a 96 well quartz plate (Molecular Devices; Sunnyvale, CA) and measuring the absorbance at 260 nm and 280 nm using a SpectraMax Plus spectrophotometer (Molecular Devices; Sunnyvale, CA). cDNA for each RNA sample (2 μg input) was generated using the High Capacity cDNA Reverse transcription kit (Applied Biosystems; Foster City, CA) according to the manufacturer's instructions. Genes chosen for further validation were selected based upon the robustness of its expression change (| fold-change | > 1.5, $p < 0.005$) and/or relatedness to schizophrenia (Katsel et al., 2008). qPCR for the following genes were performed using TaqMan gene expression assays (Applied Biosystems; Foster City, CA) according to the manufacturer's instructions: GAPDH (Mm99999915_g1), Cdkn1a (Mm00432448_m1), Gadd45a (Mm00432802_m1), Crem (Mm01230944_g1), and Ndel1 (Mm00502730_m1). Data was collected using a 48-well MJ Minioption Personal thermal cycler (BioRad; Hercules, CA). Each sample was assayed in triplicate. For relative quantification of mRNA expression, geometric means were calculated using the comparative $2^{-\Delta\Delta Ct}$ method, with the housekeeping gene GAPDH used as the endogenous reference.

## BDNF ELISA

S1 cortex was isolated from adult WT and SR−/− mice as described above and stored at −80°C until analysis. Tissue was sonicated in a 20mM Tris-HCl (pH 8.0) lysis buffer containing: 137mM NaCl, 1mm EDTA, 1% Igepal CA-630 (equivalent to NP-40), 10% glycerol, 10 μg/ml aprotinin, 0.5ug/ml antipain, 0.1ug/ml pepstatin A, and 1mM phenylmethanesulfonyl fluoride (Sigma Alrdich; St. Louis, MO), as well as phosphatase inhibitors (cocktails A and B, 1% v/v; Santa Cruz Biotechnology; Santa Cruz, CA). Samples were centrifuged at 16,000*x*g for 10 min at 4°C. The supernatant was collected and used for the quantification of total protein (BCA Protein Assay kit; Pierce; Rockford, IL) and free mature BDNF levels. BDNF levels were measured using a commercially available ELISA kit (Promega; Madison, WI) according to the manufacturer's instructions, except that the BDNF standards were diluted in tissue lysis buffer. The absorbance of the 96-well plate was read at 450 nm using a Spectramax Plus plate reader (Molecular Devices; Sunnyvale, CA).

### Western blot analysis

Western blot analyses were performed on the same samples that were used for the BDNF ELISA. Prior to gel loading, samples were heated to 95°C for 5 minutes. Equal amounts of protein (20 μg) were electrophoretically separated on an SDS-10% polyacrylamide gel. Nitrocellulose membranes (Bio-Rad, Hercules, CA) were blocked with 5% nonfat dry milk (Shaw's; Boise, ID) in 0.05% Tween-20/Tris buffered saline, cut in half, and then incubated with primary antibody overnight at 4°C. The primary antibody mouse anti-TrkB (BD Transduction Laboratories) was used at a dilution of 1:1K and rabbit anti-p-actin (Abcam; Cambridge, MA) was used at 1:8K. After incubation with rabbit anti-mouse (1:3K; Abcam, Cambridge, MA) or goat anti-rabbit (1:5K; Abcam, Cambridge, MA) horseradish peroxidase-conjugated secondary antibodies, immunocomplexes were visualized by chemiluminescence using Western Lightning-ECL (Perkin Elmer; Waltham, MA). Semi-quantitative assessment of protein bands on developed autoradiography film (Midsci, St Louis, MO) was executed by computerized densitometry on a MacIntosh G4 computer (Apple, Cupertino, CA) using Quantity One Quantitation Software (Bio-Rad, Hercules, CA). Only the protein band of ~140kDa, which corresponds to the full-length TrkB receptor was analyzed. Each sample was run in duplicate and the mean optical density (OD) of the two bands was used as the value for that sample. TrkB OD values were divided by their corresponding β-actin OD values. The mutant values were normalized to WT values (% control) collected in parallel from the same gel. The normalized values were then averaged and used for statistical analysis.

### Statistical analyses

The effect of genotype on total dendritic length and segment analyses, as well as cortical volume and PMBSF area was analyzed using two-tailed, unpaired Student's t test. Dendritic complexity was analyzed using two-factor ANOVA with repeated measures, while spine density and maturity were compared using two-factor ANOVA. Significant F tests were followed up with Student's t test comparisons. For Western blot, BDNF ELISA, and qPCR analyses, statistical differences between genotypes were determined using unpaired Student's t-test. Values of $p < 0.05$ were considered statistically significant.

## Results

### Dendritic morphology is altered in S1 cortex of SR−/− mice

In S1, the apical dendrites of pyramidal neurons were less complex in SR−/− mice (Fig. 1B; distance from soma: $F(12,71) = 116.3$, $p < 0.0001$; genotype: $F(1,71) = 12.27$, $p = 0.0008$; distance x genotype: $F(12,71) = 4.726$, $p < 0.0001$) than in WT mice. These reductions were statistically significant at distances of 40–60 μm from the soma. Moreover, the total length of apical dendrites was significantly shorter in the SR−/− as compared to WT mice (Fig. 1C; $t(71) = 3.71$, $p = 0.0004$). The characteristics of basal dendrites of neurons in SR−/− mice were also significantly affected. They were significantly less complex than those in WT mice (Fig. 1D; distance from soma: $F(10,71) = 165.2$, $p < 0.0001$; genotype: $F(1,71) = 4.17$, $p = 0.045$; distance x genotype: $F(10,71) = 2.02$, $p = 0.03$), but only at distances 40–50 μm from the soma. The total amount of basal dendritic material was also lower in the neurons of SR−/− mice (Fig. 1E; $t(71) = 2.21$, $p = 0.03$).

Segment analysis (Table 1) revealed that the dendritic perturbations were concentrated in higher order branches. In the apical system, the total length of 6th order dendrites ($t(69) = 3.20$, $p = 0.002$), the number of 4th ($t(69) = 2.26$, $p = 0.03$), 5th ($t(69) = 2.80$, $p = 0.007$), and 6th ($t(69) = 3.83$, $p = 0.0003$) order dendrites, and the average length of 6th ($t(69) = 2.70$, $p = 0.009$) and 7th ($t(69) = 2.18$, $p = 0.03$) order dendrites was lower in SR−/− mice. In the basilar system, the total length of 2nd order dendrites ($t(69) = 3.15$, $p = 0.002$), the

number of 3rd order dendrites (t(69) = 2.15, p = 0.03), and the average length of 3rd (t(69) = 3.39, p = 0.001) and 4th (t(69) = 2.40, p = 0.02) order dendrites was lower in SR−/− mice.

### Spine density is reduced in S1 cortex of SR −/− mice, with no change in spine maturity

Pyramidal neurons from SR−/− mice exhibited reductions in apical spine density on the distal portions of their apical dendrites and on oblique apical branches (Fig. 2B; genotype: F(1,31) = 11.48, p = 0.002; branch x genotype: F(1,31) = 1.79, p = 0.19). The distal sections of the primary dendrites exhibited higher spine density than the oblique branches (branch type: F(1,31) = 11.41, p = 0.002). In addition, the spine density on basal dendrites across all branch orders was significantly lower in SR−/− mice (Fig. 2C; branch order: F(2,25) = 20.02, p < 0.0001; genotype: F(1,25)= 7.20, p = 0.01; branch x genotype: F(2,25) = 0.27, p = 0.77).

The effect of NMDAR hypofunction on spine maturation was also examined in SR−/−mice. There were no differences between genotypes (F(1,10) = 0.03, p = 0.86) in the percentage of mature spines on either oblique branches (WT: 46%, KO: 48%) or the distal portion of the main apical shaft (WT: 51%, KO: 51%). There was also no overall difference in the proportion of mature spines in the different apical compartments (F(1,10) = 0.86, p = 0.37).

### Cortical volume is reduced in SR−/− mice, without alteration in gross PMBSF morphology

The volume of the cortex as a whole was stereologically estimated and compared between genotypes. SR−/− mice had significantly less (3.5%) cortical volume than WT controls (Fig. 3A; (t(35) = 2.82, p = 0.03). Due to the previously observed dendritic abnormalities in S1 of the SR−/− mice, we investigated gross barrel morphology of the posteromedial barrel subfield (PMBSF) in S1. The formation and patterning of barrels in the PMBSF were not compromised in SR−/−mice (Fig. 3B). Moreover, by measuring the area of and between barrels (Fig. 3C, D), we did not find differences in either the intra- (t(16) = 0.93, p = 0.37) or interbarrel (t(16) = 0.03, p = 0.98) areas of rows D and E between WT and SR−/− mice .

### Global gene expression changes in the S1 cortex of SR−/− mice

Analysis of microarray data using dChip software revealed 354 significant gene expression changes between WT and SR−/− mice in S1 cortex (Table S1). We validated four of the most robustly affected genes identified from the microarray analysis by qPCR from an independent group of WT and SR−/− mice (Table 2). Based on the significant gene expression changes identified in dChip, IPA software was used to gain insight into network and cellular functions that are preferentially affected in SR−/− mice. The diseases and disorders most significantly associated with the observed gene changes in SR−/− mice include psychological, genetic, and neurologic disorders (Fig. 4A). The most affected molecular and cellular functions included cell death, cellular growth, proliferation and development, cell cycle, and cell morphology (Fig. 4B). With regard to physiological system development and function, SR−/− mice displayed gene expression changes consistent with altered hematological, nervous, behavior, and embryonic development (Fig. 4C).

One notable gene expression change identified in the microarray was reduced expression of BDNF (probe set 1422168_a_at: fold-change = −1.38, p = 0.01; probe set 1422169_a_at: fold-change = −1.47 p = 0.003). Using the Pathway Designer function in IPA, we created a network of molecules that are directly and indirectly related to BDNF signaling based on the significant gene expression changes found in SR−/− according to the microarray (Fig. 5A). We found changes in the expression of several genes associated with regulating actin dynamics, including TNS1 (tensin 1), MYO6 (myosin VI), and MYH14 (myosin, heavy chain 14, non-muscle). Other notable changes included a down-regulation of adenylate

cyclase signaling (ADCY8, ADCYAP1 or PACAP) and up-regulation of mitogen activated kinase (MAPK; group) signaling.

### BDNF protein is reduced in the S1 cortex of SR−/− mice

Given the important role BDNF plays in neuronal maturation and because its expression was reduced at the mRNA level in the gene microarray, we further pursued the question of altered BDNF expression by measuring BDNF protein levels in WT and SR−/− mice. We found that mature BDNF protein was significantly reduced in the S1 region of SR−/− mice (Fig. 6A; $t(11) = 2.32$, $p = 0.04$). To gain a more complete of picture of BDNF signaling, we also measured levels of its high affinity receptor, TrkB, from the same samples used to measure BDNF. We found no significant differences in the total amount of TrkB protein (Fig. 6B; $t(12) = 0.10$, $p = 0.92$).

### GlyT1+/− mice have increased dendritic spine density in the S1 cortex

In an effort to determine whether dendritic plasticity could be bi-directionally regulated by NMDAR function, we reconstructed pyramidal neurons in GlyT1+/− mice, which display NMDAR hyperfunction (Martina et al., 2005; Tsai et al., 2004). As shown in Fig. 7A–B,D–E, there were no significant differences between pyramidal neurons from WT and GlyT1+/− mice with respect to dendritic complexity (apical: distance from soma: $F(14,29) = 47.6$, $p < 0.0001$; genotype: $F(14,29) = 0.68$, $p = 0.42$; distance x genotype: $F(14,29) = 0.82$, $p = 0.065$; basal: distance from soma: $F(11,28) = 171.6$, $p < 0.0001$; genotype: $F(11,28) = 0.03$, $p = 0.87$; distance x genotype: $F(11,28) = 0.65$, $p = 0.79$) or total dendritic length ($t(29) = 1.66$, $p = 0.25$; basal: $t(29) = 0.03$, $p = 0.97$). However, pyramidal neurons in S1 from GlyT1+/− mice did have increased spine density on both oblique apical branches and the distal apical dendrite (Fig. 7C; genotype: $F(1,29) = 4.80$, $p = 0.037$). The distal sections of the primary dendrite also had a higher spine density than the oblique branches (branch type: $F(1,29) = 26.6$, $p < 0.0001$). However, there were no significant changes in basilar dendritic spine density between genotypes (Fig. 7F; $F(1,28) = 1.24$, $p = 0.28$).

## Discussion

Over the past two decades, it has become evident that NMDAR hypofunction plays a role in the pathophysiology of schizophrenia (Coyle, 2006; Lisman et al., 2008). Moreover, there are morphological alterations in the brains of schizophrenic patients, most notably reductions in the complexity of dendritic branching, total dendritic length, and dendritic spine density of pyramidal neurons in cortical regions (Selemon and Goldman-Rakic, 1999). Our data demonstrate that in SR−/− mice, in which NMDAR signaling is hypofunctional (Basu et al., 2009), pyramidal neurons in the somatosensory cortex exhibit dendritic dysplasia that is associated with reduced cortical volume. Moreover, the gene expression profile from S1 of SR−/− mice suggests an overall dysregulation in neurodevelopment and gene changes associated with cell death and neurologic disorders. BDNF expression is also reduced in the S1 cortex of SR−/− mice. Finally, GlyT1+/− mice, which display NMDAR hyperfunction, have S1 pyramidal neurons with an increased number of dendritic spines.

The cerebral cortex is the brain region most extensively subject to neuronal dendritic analysis in *postmortem* studies of schizophrenia. In deep layer 3 of the DLPFC of subjects with schizophrenia, neurons showed reductions in both basilar dendritic expanse and spine density, but no basilar dendritic perturbations in the primary visual cortex (Glantz and Lewis, 2000). Moreover, these morphological alterations in deep layer 3 of the DLPFC from the same patients did not extend to the basal dendrites of pyramidal neurons in layer 5 or 6 of prefrontal area 46 (Kolluri et al., 2005). In the PFC, patients had neurons with both decreased total dendritic material and complexity in their basilar system, but apical dendrites

were unaffected (Kalus et al., 2000). Pyramidal neurons in the temporal and frontal cortices of schizophrenic subjects had reduced spine density, but the apical and basal dendrites in that study were combined for analysis (Garey et al., 1998). In the subiculum, schizophrenic patients had neurons with reduced spine density and arborization of apical, but not basal dendrites (Rosoklija et al., 2000). However, neurons in the fusiform gyrus from the same subjects had normal apical and basal dendritic characteristics (Rosoklija et al., 2000). Others have also found decreased spine density and increased pyramidal packing density with no reduction in pyramidal cell number in layer 3 of primary auditory cortex (Sweet et al., 2010). The results from the current study, of reduced dendritic complexity and spine density in mice with NMDAR hypofunction, are consistent with neuropathological findings in patients with schizophrenia. The *postmortem* data from patients show that these dendritic perturbations are contained to specific cortical regions and layers (Ide and Lewis, 2010). Whether this same pattern holds true in our genetic model has yet to be determined, but since D-serine is absent throughout the brains of our SR−/− mice, it is likely that the dendritic alterations will be more generalized across the cortex. The dendritic abnormalities in SR−/− mice extend to the mPFC (DeVito et al., 2011).. In addition, the modest magnitude of reduction in cortical volume observed in SR−/− mice is similar to what has been found in human imaging studies of patients with schizophrenia (Kuperberg et al., 2003).

When first identified, SR was reported on the basis of immunocytochemical staining and primary cell culture results to be expressed exclusively in astrocytes (Wolosker et al., 1999). More recent immunocytochemical studies indicate that SR protein can also be detected in neurons (Kartvlishvily et al., 2006; Miya et al., 2008). Preliminary results, in which cell specific conditional knock-outs of SR were used to quantify its expression, indicate that at least 60 percent of cortical SR protein is localized to glutamatergic neurons whereas only 20 percent was expressed in astrocytes (Benneyworth et al., in preparation).

The complexity of dendritic branching is thought to represent the extent of neuronal connectivity. Dendritic arborization is enhanced by NMDAR-dependent neurotransmission and downstream $Ca^{2+}$ sensitive signaling pathways (Wayman et al., 2008; Wayman et al., 2006). This known pathway for activity-dependent elaboration of dendritic structure suggests that the less complex dendritic trees of cortical pyramidal neurons in SR−/− mice could be due to their constitutive NMDAR hypofunction.

More than 90% of all excitatory synapses in the central nervous system are on dendritic spines (Fiala et al., 2002). Therefore, the reduced spine density of pyramidal neurons in the cortex of SR−/− mice would be expected to lead to abnormalities in glutamatergic transmission (Fiala et al., 2002). While the reductions in total dendritic length (−22%) and in overall spine density (−23%) for the basilar dendrites may seem modest, in aggregate these represent a ~40% absolute reduction in excitatory synapses. Our laboratory has previously shown that NMDAR-dependent glutamatergic transmission is perturbed in SR−/− mice (Balu and Coyle, 2011a; Basu et al., 2009). The converse electrophysiological properties have been found in the hippocampus of GlyT1+/− mice (Martina et al., 2005; Tsai et al., 2004). Future studies should shed light on potential electrophysiological alterations specifically in the S1 of SR−/− and GlyT1+/− mice. In addition, as excitatory activity influences the density of dendritic spines (Zito et al., 2009), reduced NMDAR-dependent signaling in the SR−/− mice could be responsible for the reductions in spine density, while augmented NMDAR transmission in GlyT1+/− mice could be responsible for the increased spine density.

Given this evidence that the spine density appears to be inversely related to NMDAR function, it is conceivable that the reduced spine density and even the reduced dendritic

complexity observed in the SR−/− mice could be reversed by treatment with exogenous D-serine. Since SR−/− results in loss of D-serine throughout brain development, it is unclear if there might be a “critical period” for such an intervention. Preliminary results with a conditional knock-out of SR that is activated in early adulthood (unpublished observations) suggest that the spine deficits can develop at this late stage and thus might be reversible with post-natal D-serine treatment.

The barrel field in the rodent somatosensory cortex processes sensory information arriving from the mystacial vibrissae and is organized into functional, vertically oriented columns. These columns contain excitatory and inhibitory interneurons distributed over six laminae that are connected both within and between cortical layers (Woolsey, 1996). The extent of their dendritic arbor and number and location of synaptic contacts of excitatory neurons determine the flow of excitatory signals in the cortical column (Lubke and Feldmeyer, 2007). The reduced dendritic complexity and spine density of apical and basal dendrites of pyramidal neurons in SR−/− mice suggest that signaling could be compromised within this microcircuit. Pyramidal neurons in this study were pooled from layer 2/3 (L2/3) and L4. L4 spiny neurons are the principal target of thalamic input and innervate L2/3 pyramidal cells, which in turn innervate other L2/3 or L5B pyramidal neurons. L5B neurons are a class of output neurons with axonal projections to various subcortical regions, including the thalamus and brain stem. In addition to having reduced signaling within cortical microcircuitry, SR−/− mice could potentially have reduced output signaling through L5B neurons. This type of dysfunction would be consistent with attenuated cortical event related potentials observed in schizophrenic subjects with sensory stimuli (Doniger et al., 2002).

The discrete lamina IV barrels comprising the somatotopic map in the S1 cortex are in a one-to-one relationship with the sensory vibrissae on the rodent’s muzzle (Woolsey and Van der Loos, 1970). Previous genetic studies using mice with various deletions of the NR1 subunit (Datwani et al., 2002; Iwasato et al., 2000; Iwasato et al., 1997) demonstrated that NMDAR function is necessary for proper pattering in the S1 cortex. The normal barrel patterns in our SR−/− mice are likely due to the more modest effect that co-agonist depletion has on NMDAR function as compared to the deletion of the essential NR1 subunit.

In *postmortem* studies, BDNF mRNA and protein (Hashimoto et al., 2005b; Weickert et al., 2003; Wong et al., 2010) levels are reduced in the dorsolateral PFC (DLPFC) of subjects with schizophrenia. On the other hand, the status of TrkB expression in schizophrenia is less well defined. TrkB mRNA was decreased in the PFC of subjects with schizophrenia (Hashimoto et al., 2005b; Weickert et al., 2005), while another study found no difference in the amount of TrkB protein (Takahashi et al., 2000). BDNF regulates a vast array of processes, including neurite outgrowth and spine density, by signaling through its high-affinity receptor, TrkB (Binder and Scharfman, 2004). The three major intracellular signaling pathways activated by TrkB receptors are: the Ras-MAPK pathway, PI3K–Akt pathway, and the phospholipase Cy1 (PLCyl)-$Ca^{2+}$ pathway (Huang and Reichardt, 2003). Our gene expression data suggest that MAPK signaling could be altered in SR−/− mice, as the expression of MAPK12 was increased, suggesting a compensatory mechanism to reduced BDNF levels.

Another pathway potentially altered in SR−/− mice that is connected to BDNF is PACAP signaling, because PACAP expression was reduced in SR−/− mice. PACAP is a neuropeptide expressed in the brain that regulates neurotransmission, can transactivate Trk receptors via binding to one of its three cognate G-protein-coupled receptors, and has been linked to schizophrenia (Moody et al., 2011). PACAP itself has also been reported to enhance BDNF expression in cortical neurons via potentiation of NMDAR signaling (Pellegri et al., 1998). Furthermore, recent evidence suggests that PACAP signaling

modulates DISC1-Binding Zinc-finger protein (DBZ)-DISC1 interaction, which in turn regulates DISC1-dependent neurite outgrowth (Hattori et al., 2007). Although this reduction in PACAP expression requires further validation, it highlights the potential overlap of key signaling cascades that are likely involved in the etiology of schizophrenia (Balu and Coyle, 2011b).

## Conclusions

In conclusion, pyramidal neurons in SR−/− mice displayed a small but significant reduction in cortical volume and abnormalities in spine density, arborization, and total dendritic length of S1 pyramidal neurons that was accompanied by reduced levels of BDNF. These alterations in the SR−/− mice closely mirror those reported in schizophrenia. Notably, transgenic mice for two other putative risk genes for schizophrenia, *Neuregulin-1* (Chen et al., 2010) and Disrupted in Schizophrenia 1 (*DISC1*) (Jaaro-Peled, 2009) also exhibit dendritic dysgenesis, suggesting multiple genetic pathways leading to this pathological hallmark of schizophrenia. Thus, our results suggest that NMDAR hypofunction might contribute to the dendritic and synaptic changes observed in schizophrenia and highlight the potential therapeutic benefit of GMS positive modulators not only for treating the negative and cognitive symptoms of schizophrenia but also the dendritic pathology that is likely responsible for them (Coyle, 2006; Javitt, 2006).

### Highlights

D-serine deficiency impairs NMDA receptor function and cortical dendritic plasticity

Mice lacking D-serine have reduced BDNF expression

Mice with genetically enhanced NMDA receptor function have increased spine density

## Supplementary Material

Refer to Web version on PubMed Central for supplementary material.

## Acknowledgments

We would like to thank Dr. Sabina Berretta, Dr. Francine M. Benes, and Dr. Ole Isacson for the generous use of their equipment and software. We also thank Matthew Demers, Harry Pantazopoulos, Glenn T. Konopaske, Nestor Barrezueta and Amy Truong for technical assistance, as well as Jiamin Feng for animal colony maintenance and genotyping. This work was supported by a postdoctoral National Research Service Award F32 MH090697 and an Andrew P. Merrill Research Fellowship granted to DTB, and grants R01MH05190 and P50MH0G0450, as well as an unrestricted grant from Bristol-Myers Squibb to JTC.

## References

Balu DT, Coyle JT. Glutamate receptor composition of the post-synaptic density is altered in genetic mouse models of NMDA receptor hypo- and hyperfunction. Brain Res. 2011a; 1392:1–7. [PubMed: 21443867]

Balu DT, Coyle JT. Neuroplasticity signaling pathways linked to the pathophysiology of schizophrenia. Neurosci Biobehav Rev. 2011b; 35:848–870. [PubMed: 20951727]

Bass NJ, et al. Evidence for the association of the DAOA (G72) gene with schizophrenia and bipolar disorder but not for the association of the DAO gene with schizophrenia. Behav Brain Funct. 2009; 5:28. [PubMed: 19586533]

Basu AC, et al. Targeted disruption of serine racemase affects glutamatergic neurotransmission and behavior. Mol Psychiatry. 2009; 14:719–727. [PubMed: 19065142]

Binder DK, Scharfman HE. Brain-derived neurotrophic factor. Growth Factors. 2004; 22:123–131. [PubMed: 15518235]

Chen Y, et al. Intramembranous valine linked to schizophrenia is required for neuregulin 1 regulation of the morphological development of cortical neurons. J Neurosci. 2010; 30:9199–9208. [PubMed: 20610754]

Coyle JT. Glutamate and schizophrenia: beyond the dopamine hypothesis. Cell Mol Neurobiol. 2006; 26:365–384. [PubMed: 16773445]

Datwani A, et al. NMDA receptor-dependent pattern transfer from afferents to postsynaptic cells and dendritic differentiation in the barrel cortex. Mol Cell Neurosci. 2002; 21:477–492. [PubMed: 12498788]

DeVito LM, et al. Serine racemase deletion disrupts memory for order and alters cortical dendritic morphology. Genes Brain Behav. 2011; 10:210–222. [PubMed: 21029376]

Doniger GM, et al. Impaired visual object recognition and dorsal/ventral stream interaction in schizophrenia. Arch Gen Psychiatry. 2002; 59:1011–1020. [PubMed: 12418934]

Erhardt S, et al. The kynurenic acid hypothesis of schizophrenia. Physiol Behav. 2007; 92:203–209. [PubMed: 17573079]

Fiala JC, et al. Dendritic spine pathology: cause or consequence of neurological disorders? Brain Res Brain Res Rev. 2002; 39:29–54. [PubMed: 12086707]

Fortin DA, et al. Structural Modulation of Dendritic Spines during Synaptic Plasticity. The Neuroscientist :a review journal bringing neurobiology neurology psychiatry. 2011

Galvez R, Greenough WT, et al. Sequence of abnormal dendritic spine development in primary somatosensory cortex of a mouse model of the fragile X mental retardation syndrome. Am J Med Genet A. 2005; 135:155–160. [PubMed: 15880753]

Garey LJ, et al. Reduced dendritic spine density on cerebral cortical pyramidal neurons in schizophrenia. J Neurol Neurosurg Psychiatry. 1998; 65:446–453. [PubMed: 9771764]

Glantz LA, Lewis DA. Decreased dendritic spine density on prefrontal cortical pyramidal neurons in schizophrenia. Arch Gen Psychiatry. 2000; 57:65–73. [PubMed: 10632234]

Goldman AL, et al. Widespread reductions of cortical thickness in schizophrenia and spectrum disorders and evidence of heritability. Arch Gen Psychiatry. 2009; 66:467–477. [PubMed: 19414706]

Hashimoto K, et al. Reduced D-serine to total serine ratio in the cerebrospinal fluid of drug naive schizophrenic patients. Prog Neuropsychopharmacol Biol Psychiatry. 2005a; 29:767–769. [PubMed: 15939521]

Hashimoto K, et al. Decreased serum levels of D-serine in patients with schizophrenia: evidence in support of the N-methyl-D-aspartate receptor hypofunction hypothesis of schizophrenia. Arch Gen Psychiatry. 2003; 60:572–576. [PubMed: 12796220]

Hashimoto T, et al. Relationship of brain-derived neurotrophic factor and its receptor TrkB to altered inhibitory prefrontal circuitry in schizophrenia. J Neurosci. 2005b; 25:372–383. [PubMed: 15647480]

Hattori T, et al. A novel DISC1-interacting partner DISC1-Binding Zinc-finger protein: implication in the modulation of DISC1-dependent neurite outgrowth. Mol Psychiatry. 2007; 12:398–407. [PubMed: 17389905]

Huang EJ, Reichardt LF. Trk receptors: roles in neuronal signal transduction. Annu Rev Biochem. 2003; 72:609–642. [PubMed: 12676795]

Ide M, Lewis DA. Altered cortical CDC42 signaling pathways in schizophrenia:implications for dendritic spine deficits. Biol Psychiatry. 2010; 68:25–32. [PubMed: 20385374]

Iwasat T, et al. Cortex-restricted disruption of NMDAR1 impairs neuronal patterns in the barrel cortex. Nature. 2000; 406:726–731. [PubMed: 10963597]

Iwasato T, et al. NMDA receptor-dependent refinement of somatotopic maps. Neuron. 1997; 19:1201–1210. [PubMed: 9427244]

Jaaro-Peled H. Gene models of schizophrenia: DISC1 mouse models. Prog Brain Res. 2009; 179:75–86. [PubMed: 20302820]

Javitt DC. Is the glycine site half saturated or half unsaturated? Effects of glutamatergic drugs in schizophrenia patients. Curr Opin Psychiatry. 2006; 19:151–157. [PubMed: 16612195]

Javitt DC. When doors of perception close: bottom-up models of disrupted cognition in schizophrenia. Annual review of clinical psychology. 2009; 5:249–275.

Javitt DC, Zukin SR. Recent advances in the phencyclidine model of schizophrenia. Am J Psychiatry. 1991; 148:1301–1308. [PubMed: 1654746]

Kalus P, et al. The dendritic architecture of prefrontal pyramidal neurons in schizophrenic patients. Neuroreport. 2000; 11:3621–3625. [PubMed: 11095531]

Kartvlishvily E, et al. 104.Neuron-derived D-serine release provides a novel means to activate N-methyl-D-aspartate receptors. J Biol Chem. 2006; 281:14151–14162. [PubMed: 16551623]

Katsel P, et al. Abnormal indices of cell cycle activity in schizophrenia and their potential association with oligodendrocytes. Neuropsychopharmacology. 2008; 33:2993–3009. [PubMed: 18322470]

Kishi N, Macklis JD. MECP2 is progressively expressed in post-migratory neurons and is involved in neuronal maturation rather than cell fate decisions. Mol Cell Neurosci. 2004; 27:306–321. [PubMed: 15519245]

Kolluri N, et al. Lamina-specific reductions in dendritic spine density in the prefrontal cortex of subjects with schizophrenia. Am J Psychiatry. 2005; 162:1200–1202. [PubMed: 15930070]

Kristiansen LV, et al. Expression of the NR2B–NMDA receptor trafficking complex in prefrontal cortex from a group of elderly patients with schizophrenia. Schizophr Res. 2010a; 119:198–209. [PubMed: 20347576]

Kristiansen LV, et al. Expression of the NR2B–NMDA receptor subunit and its Tbr- 1/CINAP regulatory proteins in postmortem brain suggest altered receptor processing in schizophrenia. Synapse. 2010b; 64:495–502. [PubMed: 20175224]

Krystal JH, et al. Subanesthetic effects of the noncompetitive NMDA antagonist, ketamine, in humans. Psychotomimetic, perceptual, cognitive, and neuroendocrine responses. Arch Gen Psychiatry. 1994; 51:199–214. [PubMed: 8122957]

Kuperberg GR, et al. Regionally localized thinning of the cerebral cortex in schizophrenia. Archives of general psychiatry. 2003; 60:878–888. [PubMed: 12963669]

Kwon HB, Sabatini BL. Glutamate induces de novo growth of functional spines in developing cortex. Nature. 2011; 474:100–104. [PubMed: 21552280]

Lewis DA, Gonzalez-Burgos G. Neuroplasticity of neocortical circuits in schizophrenia. Neuropsychopharmacology. 2008; 33:141–165. [PubMed: 17805309]

Li C, Wong WH. Model-based analysis of oligonucleotide arrays: expression index computation and outlier detection. Proc Natl Acad Sci U S A. 2001; 98:31–36. [PubMed: 11134512]

Lisman JE, et al. Circuit-based framework for understanding neurotransmitter and risk gene interactions in schizophrenia. Trends Neurosci. 2008; 31:234–242. [PubMed: 18395805]

Lu B. BDNF and activity-dependent synaptic modulation. Learning & memory. 2003; 10:86–98. [PubMed: 12663747]

Lubke J, Feldmeyer D. Excitatory signal flow and connectivity in a cortical column: focus on barrel cortex. Brain Struct Funct. 2007; 212:3–17. [PubMed: 17717695]

Martin KP, Wellman CL. NMDA Receptor Blockade Alters Stress-Induced Dendritic Remodeling in Medial Prefrontal Cortex. Cerebral cortex. 2011

Martina M, et al. Reduced glycine transporter type 1 expression leads to major changes in glutamatergic neurotransmission of CA1 hippocampal neurones in mice. J Physiol. 2005; 563:777–793. [PubMed: 15661817]

Miya K, et al. Serine racemase is predominantly localized in neurons in mouse brain. J Comp Neurol. 2008; 510:641–654. [PubMed: 18698599]

Moody TW, et al. VIP and PACAP: recent insights into their functions/roles in physiology and disease from molecular and genetic studies. Curr Opin Endocrinol Diabetes Obes. 2011; 18:61–67. [PubMed: 21157320]

Morita Y, et al. A genetic variant of the serine racemase gene is associated with schizophrenia. Biol Psychiatry. 2007; 61:1200–1203. [PubMed: 17067558]

Pellegri G, et al. VIP and PACAP potentiate the action of glutamate on BDNF expression in mouse cortical neurones. The European journal of neuroscience. 1998; 10:272–280. [PubMed: 9753136]

Peters A, Kaiserman-Abramof IR. The small pyramidal neuron of the rat cerebral cortex. The perikaryon, dendrites and spines. Am J Anat. 1970; 127:321–355. [PubMed: 4985058]

Rajkowska G, et al. Neuronal and glial somal size in the prefrontal cortex: a postmortem morphometric study of schizophrenia and Huntington disease. Arch Gen Psychiatry. 1998; 55:215–224. [PubMed: 9510215]

Rasser PE, et al. Gray Matter Deficits, Mismatch Negativity, and Outcomes in Schizophrenia. Schizophr Bull. 2009

Rosoklija G, et al. Structural abnormalities of subicular dendrites in subjects with schizophrenia and mood disorders: preliminary findings. Arch Gen Psychiatry. 2000; 57:349–356. [PubMed: 10768696]

Sacchi S, et al. pLG72 modulates intracellular D-serine levels through its interaction with D-amino acid oxidase: effect on schizophrenia susceptibility. J Biol Chem. 2008; 283:22244–22256. [PubMed: 18544534]

Schell MJ, et al. D-serine, an endogenous synaptic modulator: localization to astrocytes and glutamate-stimulated release. Proc Natl Acad Sci U S A. 1995; 92:3948–3952. [PubMed: 7732010]

Selemon LD, Goldman-Rakic PS. The reduced neuropil hypothesis: a circuit based model of schizophrenia. Biol Psychiatry. 1999; 45:17–25. [PubMed: 9894571]

Sepulveda FJ, et al. Differential roles of NMDA Receptor Subtypes NR2A and NR2B in dendritic branch development and requirement of RasGRF1. Journal of neurophysiology. 2010; 103:1758–1770. [PubMed: 20107120]

Shi J, et al. Allelic association of G72/G30 with schizophrenia and bipolar disorder: a comprehensive meta-analysis. Schizophr Res. 2008; 98:89–97. [PubMed: 18023149]

Sweet RA, et al. Mapping Synaptic Pathology within Cerebral Cortical Circuits in Subjects with Schizophrenia. Frontiers in human neuroscience. 2010; 4:44. [PubMed: 20631852]

Tsai G, et al. Abnormal excitatory neurotransmitter metabolism in schizophrenic brains. Arch Gen Psychiatry. 1995; 52:829–836. [PubMed: 7575102]

Tsai G, et al. Gene knockout of glycine transporter 1: characterization of the behavioral henotype. Proc Natl Acad Sci U S A. 2004; 101:8485–8490. [PubMed: 15159536]

Wayman GA, et al. An activity-regulated microRNA controls dendritic plasticity by down-regulating p250GAP. Proc Natl Acad Sci U S A. 2008; 105:9093–9098. [PubMed: 18577589]

Wayman GA, et al. Activity-dependent dendritic arborization mediated by CaM-kinase I activation and enhanced CREB-dependent transcription of Wnt-2. Neuron. 2006; 50:897–909. [PubMed: 16772171]

Weickert CS, et al. Reduced brain-derived neurotrophic factor in prefrontal cortex of patients with schizophrenia. Mol Psychiatry. 2003; 8:592–610. [PubMed: 12851636]

Wolosker H, et al. Serine racemase: a glial enzyme synthesizing D-serine to regulate glutamate-N-methyl-D-aspartate neurotransmission. Proc Natl Acad Sci U S A. 1999; 96:13409–13414. [PubMed: 10557334]

Wong J, et al. Promoter specific alterations of brain-derived neurotrophic factor mRNA in schizophrenia. Neuroscience. 2010; 169:1071–1084. [PubMed: 20553817]

Woolsey TA. Barrels: 25 years later. Somatosens Mot Res. 1996; 13:181–186. [PubMed: 9110421]

Woolsey TA, Van der Loos H. The structural organization of layer IV in the somatosensory region (SI) of mouse cerebral cortex. The description of a cortical field composed of discrete cytoarchitectonic units. Brain Res. 1970; 17:205–242. [PubMed: 4904874]

Zito K, et al. Rapid functional maturation of nascent dendritic spines. Neuron. 2009; 61:247–258. [PubMed: 19186167]

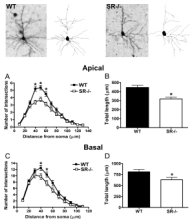


**Fig. 1.**

Pyramidal neurons in the somatosensory cortex of SR−/− mice display perturbations in apical and basilar dendritic morphology. The apical and basal dendrites of pyramidal neurons (3–8 neurons/subject) in the cortex from wild-type (WT; n= 6 mice; black) and SR −/− (n = 6 mice; white) animals were compared. Golgi stained pyramidal neurons and computer-assisted reconstructions of representative neurons in WT (left panel) and SR−/− (right panel) mice. (A), The apical dendrites of neurons from SR−/− mice were significantly less complex than WT mice between 40–60 μm from the soma. (B), The total dendritic length of neurons in SR−/− mice was significantly less than WT mice. The basal dendrites of neurons from SR−/− mice also showed significant reductions in (C), complexity (40–50 μm from the soma) and (D), total length. Asterisk (*) indicates significant difference from the WT group ($p < 0.05$). All values represent the mean ± SEM.

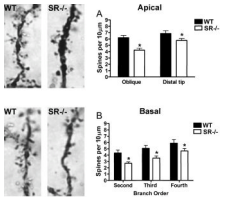


**Fig. 2.**

Reduced apical and basilar spine densities on pyramidal neurons in the somatosensory cortex of SR−/− mice. Spine density was compared between wild-type (WT; n= 6 mice; black) and SR−/− (n = 6 mice; white) animals. Apical dendritic spines on a Golgi-stained pyramidal neuron in a WT (top left panel) and a SR−/− mouse (top right panel). (A), Spine density on pyramidal neurons (3–5 neurons/subject) was reduced on both oblique branches and the distal tips of apical dendrites in SR−/− mice. Basilar dendritic spines on a Golgi-stained pyramidal neuron in a WT (bottom left panel) and a SR−/− mouse (bottom right panel). (D), Spine density on neurons (3–5 neurons/subject) was reduced across all branch orders of basal dendrites in SR−/−mice. Spine density was expressed as the number of spines per 10 μm of dendrite. Asterisk (*) indicates significant difference from the WT group ($p < 0.05$). All values represent the mean ± SEM.

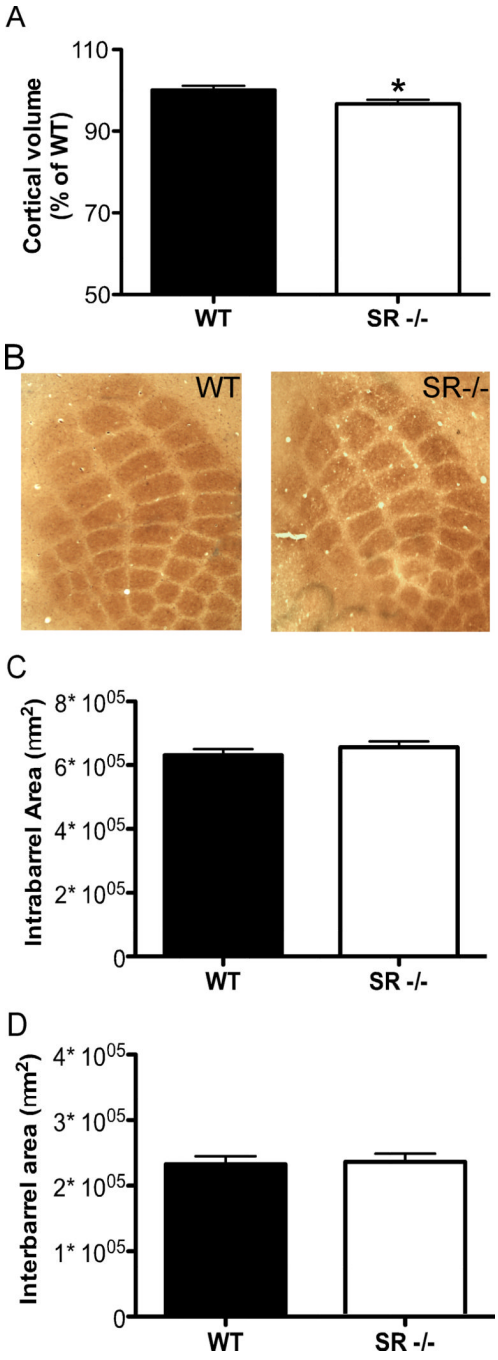


**Fig. 3.**

Cortical volume is reduced in SR−/− mice without changes in the patterning of the PSMBF. (A), The entire cortical volume was measured in wild-type (WT; n = 17; black bars) and SR −/− (n = 20; white bars) mice using stereological techniques of Nissl-stained coronal brain sections. (B), Cytochrome oxidase staining of flattened cortex was used to visualize barrels in the PMBSF of wild-type (WT; left panel) and SR−/− (right panel) mice. (C–D), The area of the barrels in each row (C) and the area between the barrel rows (D) were measured for (WT; n = 8; black bars) and SR−/− (n = 10; white bars) mice. Asterisk (*) indicates significant difference from the WT group ($p < 0.05$). All values represent the mean ± SEM.

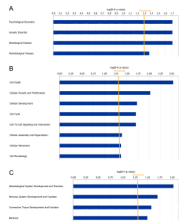

**Fig. 4.**

Network and cellular function changes in the S1 cortex of SR−/− mice following posthoc analysis of microarray gene expression data. Microarray gene expression data were obtained from wild-type (WT) and SR−/− mice (n = 6/genotype). Genes that showed significant expression changes in SR−/− mice were input into Ingenuity Pathway Analysis (IPA) software for functional analysis. (A–C) Bars represent the level of significance for each category with respect to diseases and disorders (A), molecular and cellular functions (B), and physiological system development and function (C). The orange line indicates the threshold ($p < 0.05$) for significant category enrichment following correction for multiple comparisons.

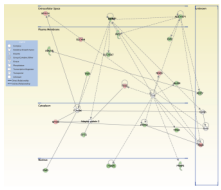

**Fig. 5.**
Graphical representation of molecules associated with BDNF whose expression is altered in SR−/− mice. Using the significant gene expression changes obtained from the microarray, IPA generated a graphical representation of the molecular relationships between molecules related to BDNF. Molecules are represented as nodes, and the biological relationship between two nodes is represented as an edge (line). The intensity of the node color indicates the degree of up- (red) or down- (green) regulation. Nodes are displayed using various shapes that represent the functional class of the gene product (see Legend). Edges are displayed with various labels that describe the nature of the relationship between the nodes.

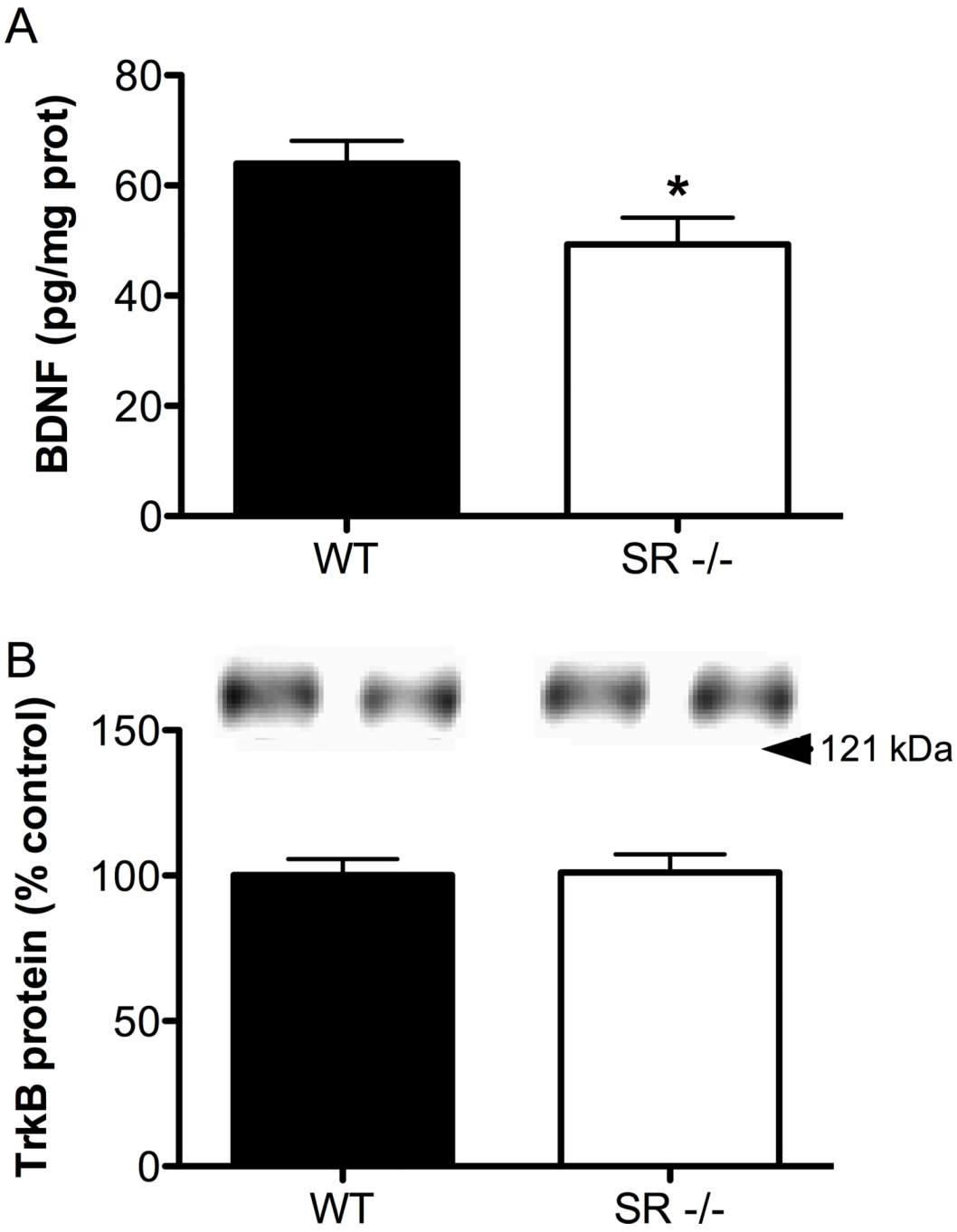


**Fig. 6.**

BDNF protein levels are reduced in the S1 cortex of SR−/− mice, without alterations in TrkB levels. (A), BNDF protein levels were measured in S1 cortex of wild-type (WT; n = 7; black bars) and SR−/− (n = 6; white bars) mice using ELISA. Values are expressed as pg of BDNF / mg of protein. (B), TrkB protein levels were measured using Western blot from the same samples used to measure BDNF. Values are expressed as the optical density (OD) normalized to WT values (% control). Asterisk (*) indicates significant difference from the WT group ($p < 0.05$). All values represent the mean ± SEM.

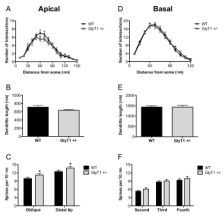


**Fig. 7.**

Pyramidal neurons in the somatosensory cortex of GlyT1+/− mice have increased apical dendritic spine density. The apical and basal dendrites of pyramidal neurons in S1 from wild-type (WT; n= 6 mice; black) and GlyT1+/− (n = 6 mice; gray) animals were compared. (A–B), There were no differences in the complexity of apical dendrites ((A)) or total apical dendritic length (B). (C), Spine density was increased in GlyT1+/− mice on both the distal portion and oblique branches of the apical dendrite. (D–F), There were no differences in the complexity of basal dendrites (D), total basal dendritic length (E), or spine density (F) of neurons from GlyT1+/− mice. Asterisk (*) indicates significant difference from the WT group ($p < 0.05$). All values represent the mean ± SEM.

**Table 1**

Detailed segment analysis of apical and basal dendrites of neurons in the S1 cortex from WT and SR−/− mice. The total length (μm), number of segments, and average length of segments (μm) were compared across each of the branch orders. *N/A* (not applicable) indicates that no data were collected at that branch order.

| | Branch Order | | | | | | |
|---|---|---|---|---|---|---|---|
| | 1st | 2nd | 3rd | 4th | 5th | 6th | 7th |
| **Total length (μm)** | | | | | | | |
| *Apical* | | | | | | | |
| WT | 14 ± 1 | 38 ± 4 | 93 ± 8 | 121 ± 11 | 84 ± 10 | 60 ± 11 | 20 ± 6 |
| SR−/− | 13 ± 1 | 44 ± 4 | 93 ± 10 | 97 ± 13 | 53 ± 13 | 14 ± 6* | 5 ± 3 |
| *Basal* | | | | | | | |
| WT | 81 ± 6 | 185 ± 17 | 273 ± 23 | 199 ± 20 | 39 ± 8 | *N/A* | *N/A* |
| SR−/− | 77 ± 8 | 144 ± 12 | 167 ± 22* | 157 ± 24 | 58 ± 14 | *N/A* | *N/A* |
| **Number of segments** | | | | | | | |
| *Apical* | | | | | | | |
| WT | 1.0 ± 0.0 | 2.1 ± 0.1 | 3.7 ± 0.3 | 4.3 ± 0.3 | 3.2 ± 0.4 | 1.8 ± 0.3 | 0.7 ± 0.2 |
| SR−/− | 1.0 ± 0.0 | 2.0 ± 0.03 | 3.3 ± 0.2 | 3.3 ± 0.4* | 1.7 ± 0.4* | 0.3 ± 0.1* | 0.2 ± 0.2 |
| *Basal* | | | | | | | |
| WT | 5.3 ± 0.2 | 7.8 ± 0.4 | 9.3 ± 0.6 | 6.3 ± 0.6 | 1.7 ± 0.3 | *N/A* | *N/A* |
| SR−/− | 4.6 ± 0.3 | 6.7 ± 0.5 | 7.2 ± 0.8* | 5.5 ± 0.7 | 2.2 ± 0.4 | *N/A* | *N/A* |
| **Average segment length (μm)** | | | | | | | |
| *Apical* | | | | | | | |
| WT | 14 ± 1 | 17 ± 1 | 24 ± 1 | 28 ± 2 | 21 ± 2 | 19 ± 3 | 8 ± 2 |
| SR−/− | 13 ± 1 | 22 ± 2* | 28 ± 2 | 27 ± 4 | 16 ± 3 | 7 ± 3* | 2 ± 1* |
| *Basal* | | | | | | | |
| WT | 15 ± 1 | 23 ± 1 | 29 ± 1 | 30 ± 2 | 12 ± 2 | *N/A* | *N/A* |
| SR−/− | 16 ± 1 | 22 ± 1 | 22 ± 1* | 22 ± 3* | 18 ± 3 | *N/A* | *N/A* |

Asterisk (*) indicates significant difference from the WT group of the same branch order ($p < 0.05$).

## Table 2

Validation of differentially expressed genes in SR−/− mice identified by microarray analysis. Relative mRNA expression of genes obtained from the S1 cortex of an independent group of wild-type (WT; n=4–6) and SR−/− (n=4–6) mice was measured by qPCR. Data is expressed as geometric means ± SEM of individual expression values normalized to the housekeeping gene GAPDH using the comparative $2^{-\Delta\Delta Ct}$ method.

| | WT | SR−/− | |
|---|---|---|---|
| | Relative mRNA expression (%WT) | | p |
| **Cdkn1a** (n = 6/genotype) | 100 ± 14 | 65 ± 5* | 0.036 |
| **Gadd45a** (n = 6/genotype) | 100 ± 15 | 58 ± 3* | 0.016 |
| **Crem** (n = 6/genotype) | 100 ± 6 | 81 ± 6* | 0.031 |
| **Ndel1** (n = 4/genotype) | 100 ± 11 | 106 ± 8 | 0.69 |

Asterisk (*) indicates significant difference from the WT group ($p < 0.05$).